chemistry proceedings

MDPI

Proceeding Paper

New Half Metal Perovskite $NbScO_3$ for Spintronic Sensing Applications †

Amall Ahmed Ramanathan

Department of Physics, The University of Jordan, Amman 11942, Jordan; amallahmad@gmail.com

† Presented at the 1st International Electronic Conference on Chemical Sensors and Analytical Chemistry, 1–15 July 2021; Available online: https://csac2021.sciforum.net/.

Abstract: Half-metallic ferromagnetic (HMF) materials demonstrate 100% spin polarization at the Fermi level, making them promising candidates for spintronic sensing applications. In this work, the full potential linearized augmented plane wave (FP-LAPW) density functional theory (DFT) method is used to calculate the electro-magnetic properties of the transition metal perovskite $NbScO_3$ using the generalized gradient approximation (GGA) and the modified Becke-Johnson (mBJ) approximation for the exchange correlations. The electronic band structures for the two spin orientations using GGA, predict $NbScO_3$ to be an HMF with an integer magnetic moment of 2.0 μB and hence a promising candidate for spintronics. The new half metal perovskite shows metallic behavior in the majority spin and semiconducting in the minority spin channel with a direct Γ−Γ band gap of 1.870 eV. The integer magnetic moment of 2.0 μB is also preserved with mBJ exchange potential. The band structure, however, shows indirect gaps R−Γ and X−Γ of 2.023 eV and 0.780 eV in the minority and majority channels, respectively indicating $NbScO_3$ to be a magnetic semiconductor. The results indicate the suitability of $NbScO_3$ for spintronics as the necessary conditions are satisfied.

Keywords: half metal; band structure; spintronics; sensors; information technology; perovskite

Citation: Ramanathan, A.A. New Half Metal Perovskite $NbScO_3$ for Spintronic Sensing Applications. *Chem. Proc.* **2021**, *5*, 82. https://doi.org/10.3390/CSAC2021-10628

Academic Editor: Ye Zhou

Published: 7 July 2021

1. Introduction

The rapid technological advancements in the last decade call for smart and sustainable lifestyle management, with sensors playing a vital role [1–4]. Electron spin is fast becoming a very useful tool in sensing devices that are based on spintronics. Spintronics is a science in which the electron spin instead of the charge is used as the information carrier, providing the advantages of low energy consumption, high speed data processing and circuit integration density [5–7]. Among today's various proposed information transfer methodologies like molecular/nano electronics and quantum technologies, spintronics stands out due to the fact that it is compatible with conventional electronics making it easy to extend the existing well known electronic techniques to spintronic circuits. HMFs, due to their exceptional electronic structure, satisfy the needs for spintronic applications. The electrons of one spin direction behave as metals and those of the other spin direction act as semiconductors. Recently, quite a few new perovskites have been predicted to be half-metals [8–10].

Transition metals (TM) are of special interest, and a variety of interesting magnetic properties have been identified, as seen from recent research results. Depending upon the local environment non-magnetic materials have become magnetic due to their presence [11–13]. TM perovskites have piqued the interest of the scientific community due the intriguing nature of the TM ion interplay with the oxide or halide ion [14,15] with the great possibilities of different electronic and magnetic properties.

Unlike the majority of previous research, wherein the TM occupies the B site, in this work we switched the sites, and the TM Niobium occupies the A site with some very interesting magneto-electronic results. The purpose of the paper is to give the essential and accurate theoretical characterization using DFT_FP-LAPW of the perovskite $NbScO_3$ which is being investigated for the first time for potential use in spintronics and sensing.

2. Method and Materials

The full-potential linearized-augmented plane wave (FP-LAPW) method, as implemented in the WIEN2k [16] package, is used to calculate the spin polarized ground states of the cubic perovskite $NbScO_3$ within the DFT [17,18] formalism. The Perdew, Burke and Ernzerhof (PBE) [19] generalized gradient approximation (GGA) is used to calculate the optimized structures for a $10 \times 10 \times 10$ k-point grid. The optimized lattice constant value is then used to evaluate the electronic and magnetic properties with the more accurate mBJ exchange correlation of Trans Blaha [20] at a denser k-point grid of $15 \times 15 \times 15$. $K_{max,}$ which provides the magnitude of the largest K vector in the plane-wave expansion is set to 8. The muffin-tin radii were set to 1.60 a.u for Sc and O atoms and 2.7 a.u for Nb. The tetrahedron method [21] with 120 k points in the irreducible Brillouin zone is employed for integrations within the self-consistency cycle (SCF). The convergence tolerance thresholds for SCF is less than 10^{-4} Ry for energy and 10^{-4} for electron charges.

3. Results and Discussion

3.1. Structural and Electronic

The cubic $NbScO_3$ perovskite has the space group Pm-3m (#221) symmetry, and the atoms occupy the positions 1a (0, 0,0), 1b ($\frac{1}{2}$, $\frac{1}{2}$,$\frac{1}{2}$) and 3c (0,$\frac{1}{2}$, $\frac{1}{2}$) sites of Wyckoff coordinates for Nb, Sc and O atoms, respectively, as depicted in Figure 1 in an inset image.

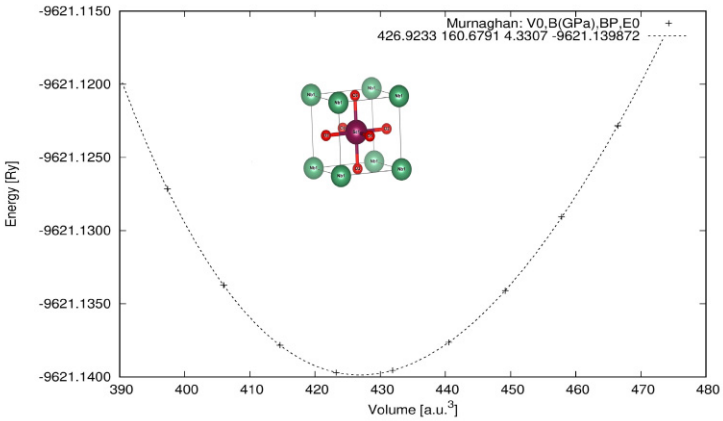

Figure 1. The energy-volume optimization and Murnaghan fit for the perovskite $NbScO_3$.

The lattice constants are optimized using the Murnaghan equation of state [22] with only volume optimization as the structure is cubic is required. The energy vs. volume optimization gives the minimum equilibrium energy state lattice parameter and is presented in Figure 1. The optimized values of the lattice constant and bulk modulus obtained are 3.985 Å and 160.679 GPa, respectively. This lattice constant value of $NbScO_3$ is used alongside the GGA-PBE and mBJ exchange correlations at denser grids to calculate the electronic band structures along the high symmetry points. The GGA band structure is shown in Figure 2 for both the spin Dn (minority) and spin Up (majority) orientations.

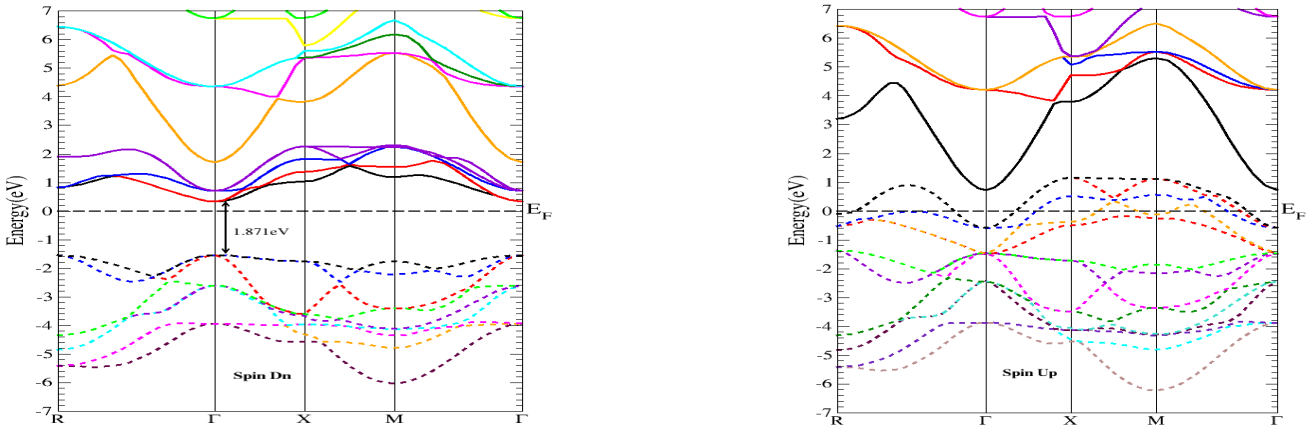

(**a**) (**b**)

Figure 2. The $NbScO_3$ electronic band structures for (**a**) the minority (Spin Dn) and (**b**) the majority (Spin Up) channels with PBE-GGA.

We see from the figure that $NbScO_3$ shows typical semi-conducting behavior in the minority spin with a direct $\Gamma-\Gamma$ gap of 1.87 eV, and that it is metallic in the majority spin resulting in a half metal ferromagnetic behavior (HMF). HMFs have 100% spin polarization and can intrinsically provide single-spin channel electrons, which are very useful in spintronics.

The band structure of $NbScO_3$ with the mBJ exchange potential on the other hand shows it to be a magnetic semiconductor as seen from the Figure 3 plots for the spin Dn and spin Up states.

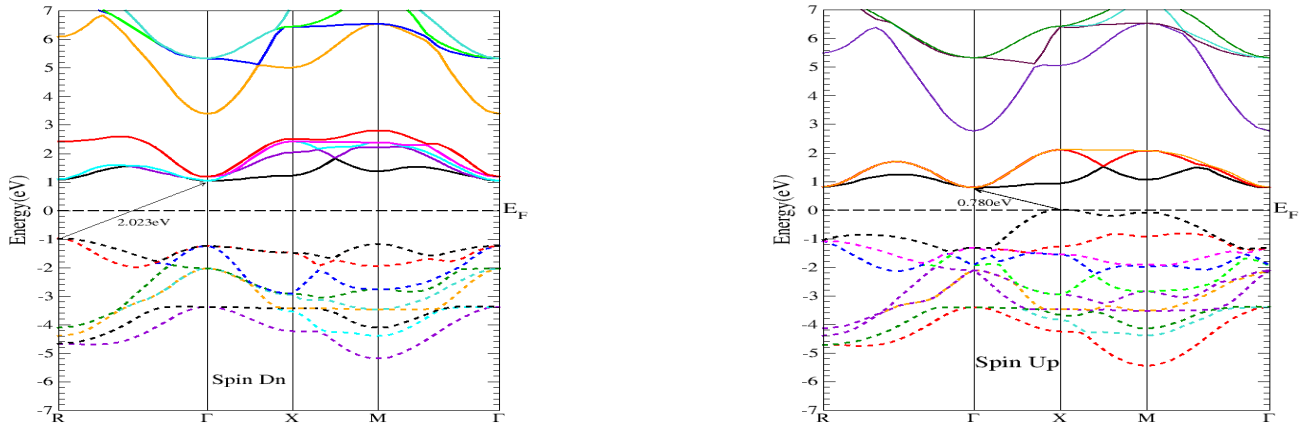

(**a**) (**b**)

Figure 3. The $NbScO_3$ electronic band structures for (**a**) the minority (Spin Dn) and (**b**) the majority (Spin Up) channels with mBJ.

The minority spin and majority spin have indirect $R-\Gamma$ and $X-\Gamma$ gaps of 2.02 and 0.78 eV, respectively. Magnetic semiconductors combine the advantages of both magnets and semiconductors, and form the basis for spintronics. Magnetic semiconductors can be used for spin generation, injection, and spin manipulation and detection. Since the mBJ exchange potential provides very reliable and accurate band structures in comparison to that of GGA or hybrid functionals, the correct behavior of $NbScO_3$ would be a magnetic semiconductor.

The half metal gap or spin flip energy E_{HM} is defined here as the minimum energy required to flip a minority-spin electron from the valance band maximum to the majority

spin Fermi level. The predicted band gaps and E_{HM} for the GGA and mBJ exchange potential are listed in Table 1.

Table 1. The electronic band gaps in the minority and majority spin channels for the $NbScO_3$ perovskite.

$NbScO_3$ Perovskite	Band Gap (eV)				E_{HM} (eV)
	Minority (Spin Dn)		Majority (Spin Up)		
GGA-PBE	Γ−Γ	1.871	metallic	No gap	1.547
mBJ	R−Γ	2.023	X−Γ	0.780	0.979

3.2. Magnetic

The band-structure plots in the previous section have clearly shown the magnetic nature of $NbScO_3$, and to fully understand the origin and hybridization of the atomic orbitals, the total and partial density of states (TDOS/PDOS) are calculated using the mBJ exchange potential. These are depicted in Figure 4.

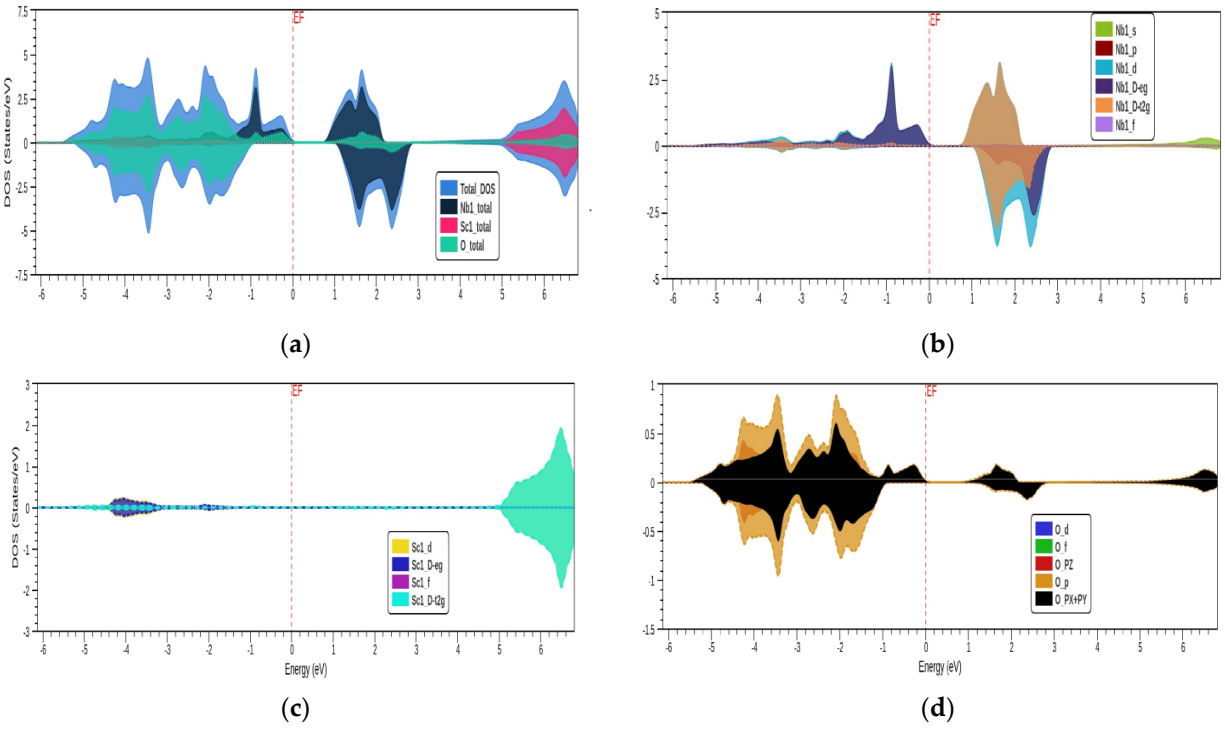

Figure 4. The $NbScO_3$ electronic DOS in both minority (bottom part) and majority (top part) spin channels (**a**) the TDOS for the compound and the atom constituents (**b**–**d**) show the PDOS in the different orbitals for the Nb atom, the Sc atom and the oxygen atom, respectively.

We can clearly observe the semiconducting and magnetic nature of $NbScO_3$from the plots. The minority channel shows the wide band gap, with no states at E_F (Fermi-energy), whereas the majority channel has the valence band edge at the Fermi energy and one can say that $NbScO_3$ is an intrinsic magnetic semiconductor. The role of Sc in the magnetism is negligible as indicated by the spin polarized PDOS plot for Sc. The main contribution to the magnetism comes from the 'd' orbital of Nb and the 'Px' and 'Py' orbitals of O_2. Additionally, the significant difference in the majority and minority TDOS can be clearly seen; resulting in the total integer magnetic moment of 2 μB typical of HMF as given in Table 2. The table also lists the atom-wise and interstitial magnetic moments of $NbScO_3$ with the GGA and mBJ exchange correlations.

Table 2. The total and atom projected magnetic moments of the $NbScO_3$ perovskite in units of μ_B.

Exchange	Nb	Sc	O	Intertitial	Total Moment
GGA_PBE	1.8484	0.0126	−0.0761	0.3673	2.0000
mBJ	1.7095	−0.0007	0.0460	0.1533	2.0000

4. Conclusions

In conclusion, the FP-LAWP investigation of the perovskite $NbScO_3$ has predicted the system to be a HMF and an intrinsic magnetic semiconductor using the GGA and mBJ exchange potentials, respectively. Moreover, the considerable size of the bandgap and magnetic moment obtained confirms the feasibility of $NbScO_3$ for spintronic applications. In addition, the large value of E_{HM} supports the robustness of this system for spintronics and sensing applications, whereby a significant role is played by the spin of the electrons in the sensor design.

Funding: This research no external funding.

Institutional Review Board Statement: Not applicable.

Informed Consent Statement: Not applicable.

Data Availability Statement: Data can be provided upon reasonable request.

Conflicts of Interest: The authors declare no conflict of interest.

References

1. Tricoli, A.; Nasiri, N.; De, S. Wearable and miniaturized sensor technologies for personalized and preventive medicine. *Adv. Funct. Mater.* **2017**, *27*, 1605271. [CrossRef]
2. Aqra, M.W.; Ramanathan, A.A. Review of the Recent Advances in Nano-Biosensors and Technologies for Healthcare Applications. *Chem. Proc.* **2021**, *5*, 76. [CrossRef]
3. Behera, B.; Joshi, R.; Vishnu, G.K.A.; Bhalerao, S.; Pandya, H.J. Electronic nose: A non-invasive technology for breath analysis of diabetes and lung cancer patients. *J. Breath Res.* **2019**, *13*, 024001. [CrossRef] [PubMed]
4. Ramanathan, A.A. Defect Functionalization of MoS_2 nanostructures as toxic gas sensors: A review. *IOP Conf. Ser. Mater. Sci. Eng.* **2018**, *305*, 012001. [CrossRef]
5. Ramanathan, A.A. First Principles Investigation of the Optoelectronic Properties of Molybdenum Dinitride for Optical Sensing Applications. *Chem. Proc.* **2021**, *5*, 27. [CrossRef]
6. Wolf, S.A.; Awschalom, D.D.; Buhrman, R.A.; Daughton, J.M.; von Molnár, V.S.; Roukes, M.L.; Chtchelkanova, A.Y.; Treger, D.M. Spintronics: A spin-based electronics vision for the future. *Science* **2001**, *294*, 1488–1495. [CrossRef]
7. Li, X.; Yang, J. First-principles design of spintronics materials. *Natl. Sci. Rev.* **2016**, *3*, 365–381. [CrossRef]
8. Khandy, S.A.; Gupta, D.C. Structural, elastic and magneto-electronic properties of half-metallic BaNpO3 perovskite. *Mater. Chem. Phys.* **2017**, *198*, 380–385. [CrossRef]
9. He, M.S. Half-metallic double perovskites Sr2CrWO6 and Sr2FeReO6 materials for spintronics applications. *Adv. Tissue Eng. Regen. Med. Open Access* **2018**, *4*, 1–6. [CrossRef]
10. Ramanathan, A.A.; Khalifeh, J.M. Electronic, magnetic and optical properties of XScO3 (X = Mo, W) perovskites. *PeerJ Mater. Sci.* **2021**, *3*, e15. [CrossRef]
11. Babar, Z.U.D.; Fatheema, J.; Arif, N.; Anwar, M.S.; Gul, S.; Iqbal, M.; Rizwan, S. Magnetic phase transition from paramagnetic in Nb2AlC-MAX to superconductivity-like dia-magnetic in Nb2C-MXene: An experimental and computational analysis. *RSC Adv.* **2020**, *10*, 25669–25678. [CrossRef]
12. Ramanathan, A.A.; Khalifeh, J.M.; Hamad, B.A. Evidence of surface magnetism in the V/Nb(0 0 1) system: A total energy pseudopotential calculation. *Surf. Sci.* **2008**, *602*, 607. [CrossRef]
13. Ramanathan, A.; Khalifeh, J.; Hamad, B. Structure and magnetism of the V/Ta(001) surface: A DFT calculation. *J. Magn. Magn. Mater.* **2009**, *321*, 3804–3807. [CrossRef]
14. Tomiyasu, K.; Okamoto, J.; Huang, H.Y.; Chen, Z.Y.; Sinaga, E.P.; Wu, W.B.; Chu, Y.Y.; Singh, A.; Wang, R.-P.; de Groot, F.M.F.; et al. Coulomb Correlations Intertwined with Spin and Orbital Excitations in LaCoO3. *Phys. Rev. Lett.* **2017**, *119*, 196402. [CrossRef] [PubMed]
15. Julian Gebhardt, J.; Rappe, A.M. Transition metal inverse-hybrid perovskites. *Mater. Chem. A* **2018**, *6*, 14560–14565. [CrossRef]
16. Blaha, P.; Schwarz, K.; Tran, F.; Laskowski, R.; Madsen, G.K.; Marks, L.D. WIEN2k: An APW+ lo program for calculating the properties of solids. *J. Chem. Phys.* **2020**, *152*, 074101. [CrossRef]
17. Ramanathan, A.A. A DFT calculation of Nb and Ta (001) Surface Properties. *JMP* **2013**, *4*, 432–437. [CrossRef]

18. Ramanathan, A.A. The Magnetism of a Ni Monolayer on Vanadium: Structure and Exchange Correlation Effects. *IEEE Trans. Nanotechnol.* **2020**, *19*, 11–16. [CrossRef]
19. Perdew, J.P.; Burke, K.; Ernzerhof, M. Generalized gradient approximation made simple. *Phys. Rev. Lett.* **1996**, *77*, 3865–3868. [CrossRef]
20. Tran, F.; Blaha, P. Accurate Band Gaps of Semiconductors and Insulators with a Semilocal Exchange-Correlation Potential. *Phys. Rev. Lett.* **2009**, *102*, 226401. [CrossRef]
21. Blöchl, P.E.; Jepsen, O.; Andersen, O.K. Improved tetrahedron method for Brillouin-zone integrations. *Phys. Rev. B* **1994**, *49*, 16223. [CrossRef] [PubMed]
22. Murnaghan, F.D. The Compressibility of Media under Extreme Pressures. *Proc. Natl. Acad. Sci. USA* **1944**, *30*, 244–247. [CrossRef] [PubMed]